

- time span simulated (fig. S6 and table S8). These results, combined with the lack of resolution within superclades of the metazoan tree, argue against models of metazoan radiation in which the temporal window of diversification is much larger (48).
39. J. A. Clack, *Gaining Ground: the Origin and Evolution of Tetrapods* (Indiana Univ. Press, Bloomington, IN, 2002).
  40. N. Takezaki, F. Figueroa, Z. Zaleska-Rutczynska, N. Takahata, J. Klein, *Mol. Biol. Evol.* **21**, 1512 (2004).
  41. Y. I. Wolf, I. B. Rogozin, E. V. Koonin, *Genome Res.* **14**, 29 (2004).
  42. J. E. Blair, K. Ikeo, T. Gojobori, S. B. Hedges, *BMC Evol. Biol.* **2**, 7 (2002).
  43. H. Philippe, N. Lartillot, H. Brinkmann, *Mol. Biol. Evol.* **22**, 1246 (2005).
  44. S. L. Baldauf, J. D. Palmer, *Proc. Natl. Acad. Sci. U.S.A.* **90**, 11558 (1993).
  45. J. L. Boore, D. Lavrov, W. M. Brown, *Nature* **393**, 667 (1998).
  46. A. Rokas, P. W. H. Holland, *Trends Ecol. Evol.* **15**, 454 (2000).
  47. A goodness-of-fit test using parametric bootstrapping (15) showed that even the best-fit model of sequence evolution does not adequately describe the evolution of the sequence data from these 32 fungal and metazoan taxa (fig. S8).
  48. G. A. Wray, J. S. Levinton, L. H. Shapiro, *Science* **274**, 568 (1996).
  49. We thank D. Arendt for providing RNA for *Platynereis dumerilii*; C. Ané for providing the modified version of the Seq-Gen simulation software with an implementation of a covarion model; and B. Prud'homme, B.

the symmetry representations correspond to even or odd parity of an energy level.

We now report the successful use of LID to deplete the population of the  $B_{2u}$  isomer in a sample of gaseous ethylene, followed by monitoring of the subsequent spin conversions for the return to equilibrium. We measured isomer concentrations by recording the absorption intensities of spectral lines with appropriate  $J$ ,  $K_a$ , and  $K_c$  quantum numbers. Our experimental setup uses two  $\text{CO}_2$  lasers (Edinburgh Instruments PL3 as the separation laser and a home-built laser as the probe) and three glass cells (for separation, test, and reference) (16). We measured the spin conversion rates for  $^{13}\text{CH}_3\text{F}$  with this setup and obtained good agreement with the published results (6, 7).

For the ethylene study, the experimental schemes are shown in Table 2, where the reported results from high-resolution infrared spectroscopy (17) were used to calculate the frequency offsets between the  $\text{C}_2\text{H}_4$  transition frequencies and the  $\text{CO}_2$  laser frequencies. Application of the LID technique for the separation of nuclear spin isomers requires that a molecular transition be near-coincident with a  $\text{CO}_2$  laser line. Here, the 10P44 laser line with a power of 6 W was used. Its frequency was tuned about 20 MHz above the center frequency by adjusting the laser cavity length to set it in the red wing of the  $9_{0,9} \leftarrow 10_{1,9}$  line of the  $\nu_7$  band of ethylene. This frequency selectively excited the  $B_{2u}$  isomer, with the other three isomers acting as a buffer gas. The  $B_{2u}$  molecules drift, by the LID effect, along the direction of the separation laser beam in the separation cell, thereby depleting the  $B_{2u}$  species and enriching the  $A_g$ ,  $B_{1g}$ , and  $B_{3u}$  species at the entrance end of the cell; this direction of drift corresponds to an increase in the collision cross section upon excitation. The nonequilibrium population was then transferred through a valve from the near end of the separation cell to the test cell. For high sensitivity, we measured differential absorption by splitting the probe beam to acquire simultaneous data from the test cell and the reference cell with a population at thermal equilibrium. We determined normalized absorption intensity differences for appropriate probe lines to

e

populations. Very similar signals were also observed for alternative  $B_{2u}$  and  $B_{3u}$  probe resonances (cases 2 and 3 in Table 2). We tried to monitor the  $B_{1g}$  population dynamics but were not successful because the line intensity of the resonant  $26_{10,16} \leftarrow 27_{9,18}$  transition was too weak. The signals in the third period show the relaxation due to the conversion among spin isomers. A model function  $A \exp(-\gamma t) + B$  (where  $A$  is the integrated intensity,  $\gamma$  is the observed conversion rate constant, and  $B$  is the baseline offset) was fitted to the decay data of Fig. 1 to give the solid smooth curve shown with a rate constant  $\gamma = 8.09 (\pm 0.10) \times 10^{-4} \text{ s}^{-1}$ .

The data clearly show that the concentration of the  $A_g$  species is almost constant in time, whereas monoexponential kinetics are observed for recovery of the depleted  $B_{2u}$  population and decay of the enriched  $B_{3u}$  population. Furthermore, the  $B_{2u}$  signal does not return to the original zero-difference baseline, and the  $B_{3u}$  signal overshoots the baseline and asymptotically approaches a new equilibrium level. These general phenomena can be qualitatively explained using Curl's theory of state mixing (19). We assume that conversion of nuclear spin isomers of  $\text{C}_2\text{H}_4$  is allowed between the  $B_{2u}$  and  $B_{3u}$  isomers, and between the  $A_g$  and  $B_{1g}$  isomers, but forbidden between species of opposite inversion symmetry. Specifically, molecular "doorway" states are posited, between either  $B_{2u}$  and  $B_{3u}$  or  $A_g$  and  $B_{1g}$ , that are so close in energy that the weak intramolecular nuclear spin-rotation and spin-spin interactions of  $\text{C}_2\text{H}_4$  can induce mixing between them. This mixing is interrupted by collisions, which promote interconversion between either the  $B_{2u}$  and  $B_{3u}$  or the  $A_g$  and  $B_{1g}$

19. R. F. Curl Jr., J. V. V. Kasper, K. S. Pitzer, *J. Chem. Phys.* **46**, 3220 (1967).  
 20. P. L. Chapovsky, *Phys. Rev. A* **43**, 3624 (1991).  
 21. Z.-D. Sun, F. Matsushima, S. Tsunekawa, K. Takagi, *J. Opt. Soc. Am. B* **17**, 2068 (2000).  
 22. We express sincere thanks to P. L. Chapovsky for valuable guidance when he visited our laboratory. We thank P. L. Chapovsky and R. M. Lees for critical

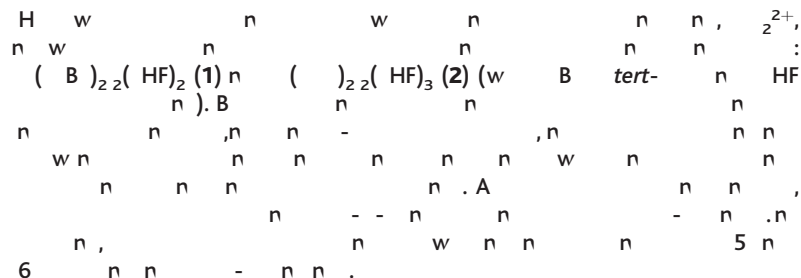
reading and commenting on the manuscript; T. Oka and J. T. Hougen for helpful discussions; Y. Moriwaki, K. Uehara, and group members for assistance in this work; and the anonymous referees for their insightful comments. Supported by the Japan Society for the Promotion of Science (JSPS) and grant-in-aid P04063 for JSPS Fellows from the Ministry of Education, Science, Sports, and Culture of Japan (Z.-D.S.).

**Supporting Online Material**  
[www.sciencemag.org/cgi/content/full/310/5756/1938/DC1](http://www.sciencemag.org/cgi/content/full/310/5756/1938/DC1)  
 Materials and Methods  
 Fig. S1

12 September 2005; accepted 27 October 2005  
 10.1126/science.1120037

# Synthesis of Imido Analogs of the Uranyl Ion

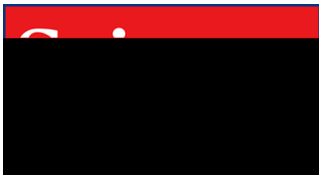
Trevor W. Hayton,<sup>1</sup> James M. Boncella,<sup>1\*</sup> Brian L. Scott,<sup>1</sup>  
 Phillip D. Palmer,<sup>1</sup> Enrique R. Batista,<sup>2</sup> P. Jeffrey Hay<sup>2</sup>



The uranyl ( $\text{UO}_2^{2+}$ ) species is the most common functional unit in the chemistry of U(VI) and has been known for more than 150 years (1). With the advent of nuclear energy and the use of uranium oxide as reactor fuel, the chemistry of the uranyl ion has played an essential role in the processing of uranium ore, nuclear fuel, and waste (2). The linear arrangement of the oxo ligands, extremely short U-O bond lengths, and high thermal and chemical stability reflect some of the unusual properties of this functional group (3). Given the prevalence of uranyl, it is surprising that metal-ligand multiple bonding in the actinides is not better understood. For instance, it is generally agreed that the uranium-oxygen bonds in uranyl involve six U-O interactions; however, the ordering of the frontier orbitals is still being debated (4). Furthermore, recent high-profile reports, such as the synthesis of a molecular uranium nitride (5) and the isolation of an  $\eta^1$ -O-bound uranium- $\text{CO}_2$  complex (6), point to a general deficiency in our knowledge of the chemistry of the f elements relative to the transition metals. The importance of multiple bonding in the actinides and the extent that the f orbitals participate in bonding are still open questions that can be addressed through the synthesis of new classes of compounds.

The imido ligand ( $\text{NR}^{2-}$ ) is isoelectronic with the oxo ligand, and the two groups can

often be interchanged in transition metal complexes. The alkyl or aryl substituent of the imido ligand provides a variable unavailable in oxo chemistry, because changes in the steric and electronic properties of the imido substituent can affect the chemistry of the metal center to which it is bound. The synthesis of the isoelectronic imido analogs of uranyl has therefore been of interest for many years (7). However, direct imido analogs of the uranyl ion have remained elusive despite a great deal of effort toward their synthesis.



**Separation and Conversion Dynamics of Four Nuclear Spin Isomers of Ethylene**

Zhen-Dong Sun, Kojiro Takagi and Fusakazu Matsushima  
(December 23, 2005)

*Science* **310** (5756), 1938-1941. [doi: 10.1126/science.1120037]

Editor's Summary

---

This copy is for your personal, non-commercial use only.

---

- Article Tools** Visit the online version of this article to access the personalization and article tools:  
<http://science.sciencemag.org/content/310/5756/1938>
- Permissions** Obtain information about reproducing this article:  
<http://www.sciencemag.org/about/permissions.dtl>

*Science* (print ISSN 0036-8075; online ISSN 1095-9203) is published weekly, except the last week in December, by the American Association for the Advancement of Science, 1200 New York Avenue NW, Washington, DC 20005. Copyright 2016 by the American Association for the Advancement of Science; all rights reserved. The title *Science* is a registered trademark of AAAS.